ISSN 2347 - 3983
Volume 11. No.12, December 2023
International Journal of Emerging Trends in Engineering Research
Available Online at http://www.warse.org/IJETER/static/pdf/file/ijeter0811122023.pdf
https://doi.org/10.30534/ijeter/2023/0811122023

Nano Conducting Particles Based Antireflection Coating for Silicon Solar Cells

R.Sharma*, A. Virdi
Model Institute of Engineering and technology (MIET), Jammu, India – 181122.
*Email: rajinder.ash@mietjammu.in

Received Date: October 25, 2023 Accepted Date: November 27, 2023 Published Date : December 07, 2023

ABSTRACT

An attempt has been made to investigate the effect of antireflection coating containing aluminum nanoparticles over the layer of silicon nitride on silicon surface. In this regard numerical calculations have been performed to obtain reflectance for varying radius (i.e., 50 nm, 62.5 nm and 70 nm) as well as periods (i.e., 100 nm, 110 nm 125 nm, 250 nm and 300 nm) of Al-NCPs using transfer matrix method (TMM). The refractive index of nanoparticles under consideration is wavelength dependent. Inclusion of metal nanoparticles in the antireflection coating has reduced reflectance significantly. Calculated reflectance has been used as an external file in PC1D simulator to study the performance of silicon solar cells.

Key words: Antireflection Coating, nano conducting particles, transfer matrix method, PC1D, silicon solar cell, conversion efficiency.

1. INTRODUCTION

Silicon technology stands as the most extensively employed material for solar cells, predominantly owing to its commendable balance between efficiency and cost-effectiveness, coupled with its remarkable reliability [1]. Nonetheless, a significant challenge confronting solar cell performance lies in the loss of light energy attributed to surface reflection. In its pristine state, silicon exhibits a notably high reflectivity, with over 30% of incident light bouncing back from its surface [2]. It is widely acknowledged that the application of one or more Anti-Reflection Coating (ARC) layers on the front surface of silicon cells mitigates this reflection, thereby enhancing device performance [2-4]. An ideal ARC can substantially curtail reflection losses across a broad spectral range. Numerous researchers have explored single- and double-layer ARCs both theoretically and experimentally. For instance, R. Sharma et al. [2] examined the effects of single and double-layer ARCs composed of various materials, while G. Hashmi et al. [5] investigated the impact of diverse ARCs using PC1D simulations. Additionally, studies by Lien et al. [6], Bahrami et al. [7], M. Medhat et al. [8], and R. Sharma [9] delved into materials like SiO2/TiO2, Al2O3/TiO2, MgF2/Ti2O3, and SiNx/SiNx, respectively.

In recent decades, significant progress has been made in employing nanoparticles to fabricate solar cell structures, owing to their exceptional light-trapping efficiency within the proposed designs. Researchers have demonstrated that strategically positioned and sized nanoparticles can effectively scatter solar radiation, substantially enhancing the performance of thin-film cells [10, 11]. Numerous studies have explored the enhancement of thin-film solar cells through scattering by gold and silver nanoparticles [12-15]. Atwater et al. took a step further by embedding metal nanoparticles inside the solar cells, capitalizing on the potent local field enhancement around these nanoparticles to boost absorption within the surrounding semiconductor material [16]. This phenomenon becomes particularly valuable in materials characterized by limited carrier diffusion lengths. Furthermore, the conversion of light into surface plasma polaritons, electromagnetic waves that travel along the interface between a corrugated metal back contact and the semiconductor absorber layer, has been investigated. These polaritons, when excited at this interface, can trap and guide light laterally into the solar cell. Given the substantial width of solar cells compared to their thickness, this approach can significantly enhance absorption, especially for long-wavelength photons.

2. STRUCTURE OF ARC

The controlled utilization of surface plasmonic resonances in metal nanostructures has garnered significant attention across various application domains, with photovoltaic devices standing as a particularly promising field. In this context, arrays of nano conducting particles (often referred to as "plasmonic layers") strategically positioned at the front surface, within the active region to amplify radiation absorption within the cell through mechanisms such as light scattering and near-field effects [17].

Figure 1 shows device structure considered for investigation comprises four regions. Region 1 is a vacuum, region 2 is filled with nano conducting particles of aluminum (Al-NPs), region 3 is a layer of silicon nitride and region 4th is of silicon. Various methods are used to calculate thereflectivity of ARCs, such as the Fresnel formula, Rouard's method, and the transfer matrix method (TMM)[18]. The transfer matrix is the most commonly usedmethod as it relates incident and reflected waves at the input layer with the incident and reflected waves

at the output layer. According to the boundary conditions, the tangential components of the electric and magnetic fields are continuous across the interface. For single layer system, field components at first boundary are related to those at second boundary by the following expressions [18, 19]:

$$E_a = E_b \cos(\delta) + B_b \left(\frac{i \sin(\delta)}{\eta}\right) \quad (1)$$

$$B_a = E_b(i\eta \sin(\delta)) + B_b \cos(\delta) \quad (2)$$

These two equations in matrix form can be expressed as [19]:

$$\begin{bmatrix} E_a/E_b \\ B_a/E_b \end{bmatrix} = \begin{bmatrix} B \\ C \end{bmatrix} = \begin{bmatrix} cos(\delta) & \frac{i\, sin(\delta)}{\eta} \\ i\eta\, sin(\delta) & cos(\delta) \end{bmatrix} \begin{bmatrix} 1 \\ \eta_s \end{bmatrix} \quad (3)$$

where $\delta = \frac{2\pi n_1 d_1 Cos\theta_1}{\lambda_o}$ is phase thickness of film, $d_1 = \frac{\lambda_o}{4n_1}$ is the thickness of film, θ_1 is the diffraction angle related to the incidence angle θ_0 by the Snell's law: $n_o\, sin\theta_o = n_1\, sin\theta_1$ and η_s is the optical admittance. Further, at normal incidence transfer matrix for double layer antireflection coating (DLARC) is [9, 19]:

$$\begin{bmatrix} B \\ C \end{bmatrix} = \begin{bmatrix} \cos(\delta_1) & \frac{i \sin(\delta_1)}{\eta_1} \\ \eta_1 i \sin(\delta_1) & \cos(\delta_1) \end{bmatrix} \begin{bmatrix} \cos(\delta_2) & \frac{i \sin(\delta_2)}{\eta_2} \\ \eta_2 i \sin(\delta_2) & \cos(\delta_2) \end{bmatrix} \begin{bmatrix} 1 \\ \eta_s \end{bmatrix} \quad (4)$$

Thus, reflectance for a given assembly can be expressed as [19].

$$R = \left| \frac{1 - \frac{Y}{n_0}}{1 + \frac{Y}{n_0}} \right|^2 \quad (5)$$

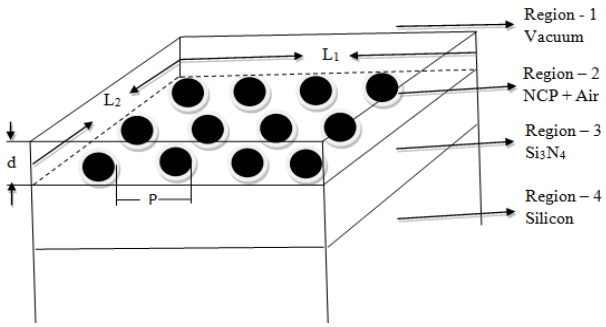

Figure 1: Antireflection coating structure containing metal nanoparticles and silicon nitride on silicon substrate.

where $Y = C/B$. The effective permittivity and refractive index of the medium of 2nd region formed by metal (aluminum) nanoparticles in air are obtained by using Maxwell-Garentt medium approximation [20]:

$$\varepsilon_i(\lambda) = \varepsilon_a \frac{\varepsilon_l(1+2f)+2\varepsilon_a(1-f)}{\varepsilon_l(1-f)+\varepsilon_a(2+f)} \quad (6)$$

$$n(\lambda) = \sqrt{\varepsilon_i(\lambda)} \quad (7)$$

where ε_a is the permittivity of base material (air), ε_l is the permittivity of the nanoparticles of aluminum and $f = (N_p \times V_p)/V_{layer}$ is the volume fraction of nano-pertcles in the base medium (air). $N_p = (L_1/P) \times (L_2/P)$ is the number of particles on the surface, $V_{layer} = L_1 \times L_2 \times d$ is the volume of the layer of thickness d (for simplicity we consider $L_1 = L_2 = 1$ cm) and $V_p = 4\pi r^3/3$ is the volume of spherical particle of radius r. Further, the permittivity of the aluminum (nanoparticle) can be calculated using Drude model as [21]:

$$\varepsilon_l(\lambda) = 1 - \frac{\lambda^2 \lambda_c^2}{\lambda_p^2(\lambda_c - i\lambda)} \quad (8)$$

where λ is the wavelength of the incident radiation, $\lambda_c = 2.4511 \times 10^{-5}$ m and $\lambda_p = 1.0657 \times 10^{-7}$ m are the collision and plasma wavelengths of the metal respectively.

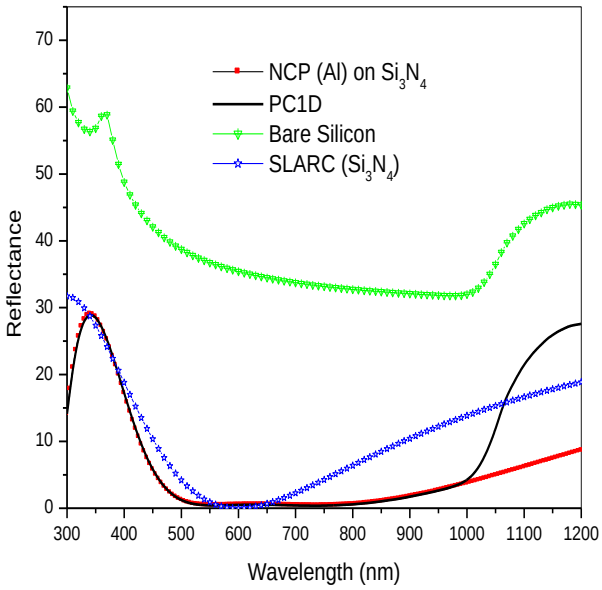

Figure 2: Plot shows variation of reflectance as function of wavelength of incident radiation.

3. RESULTS AND DISCUSSION

The characteristic reflectance curves for silicon solar cells as a function of wavelength for incident radiation at normal incident are shown in figure 2. Reflectance curves are obtained for bare silicon, for SLARC of Si_3N_4 (of thickness 60 nm and $n_2 = 2.5$) on silicon surface and for layer of Al-NPs (of radius 62.5 nm and period 250 nm) on Si_3N_4 layer and Si surface. Figure shows the reflectance for bare silicon is greater than 30% over the entire spectral range whereas SLARC (Si_3N_4) can reduce reflectance to zero corresponding to single

wavelength only (i.e., 600 nm). Further inclusion of Al-NPs over Si_3N_4 and Si surface reduces reflectance appreciably over a wide range of spectra (500 – 1000 nm).

Figure 3 shows the variation of reflectance as a function of wavelength of incident radiation with respect to the radius of Al-NPs. i.e.,*r* = 50 nm, 62.5 nm and 70 nm. The plot shows the minimum reflectance is achieved for radius 62.5 nm. Further the effect of periods of Al-NPs keeping the radius of NCPs constant at 62.5 nm is studied. Figure 4 shows the variation of reflectance as a function of wavelength of incident radiation for periods of particles 100 nm, 110 nm, 125 nm, 250 nm and 300 nm.

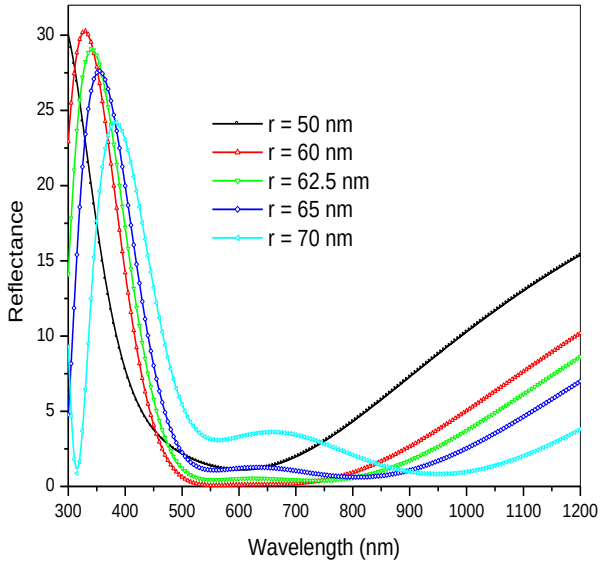

Figure 3: Plot shows variation of reflectance as a function of wavelength of incident radiation for varying radius of NCPs.

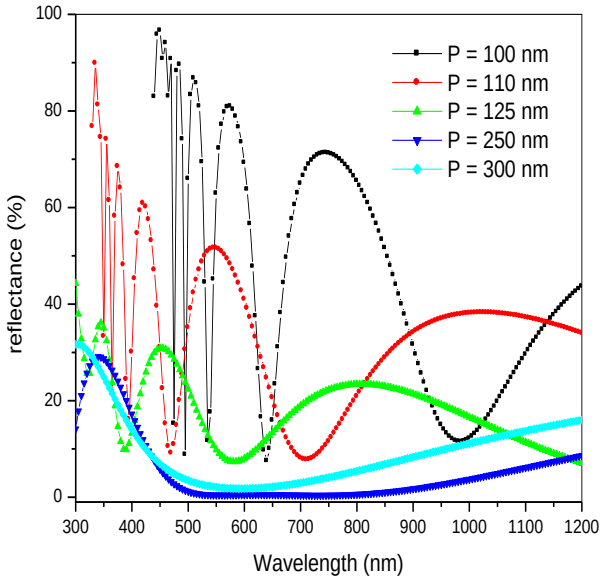

Figure 4: Plot shows variation of reflectance as a function of wavelength of incident radiations for varying periods of NCPs.

From figure one can see the behavior of reflectance is nonlinear at low periods and reflectance becomes more and more linear with increase in period of Al-NPs. For the period of 250 nm reflectance is linear as well as minimum over a wide range of spectra.

Further, the reflectance calculated above (air/Al-NPs/Si_3N_4/Si) using TMM is used in PC1D simulator to study the performance of silicon solar cells. Figure 3 shows a good agreement between the reflectance obtained from PC1D (solid line) and numerically calculated (line plus symbol). One of the important parameters of solar cells is the external quantum efficiency (EQE) which relates electrical parameters such as short circuit current and conversion efficiency to the optical parameter like reflectance. So, the performance of a solar cell can be analyzed in terms of reflectance and EQE i.e., EQE of a solar cell will be maximum when reflectance is minimum. Figure 5 presents EQE as a function of wavelength of incident radiations. Plot shows the EQE is almost 100 % over a wide range of spectra (500 – 1000 nm).

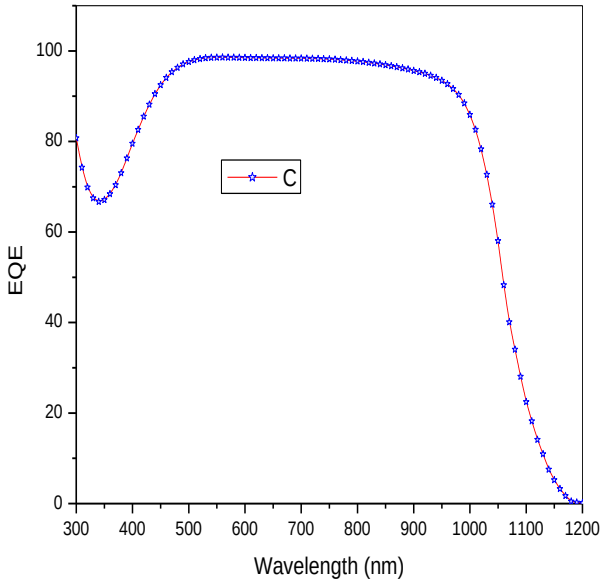

Figure 5: Plot shows variation of external quantum efficiency as a function of wavelength of light for silicon solar cells.

4. CONCULUSION

In present work we have numerically investigated the effect of antireflection coating containing Al-NPs over the layer of Si_3N_4 on the surface of silicon. The reflectance as a function of wavelength of incident radiation for particle size and period size has been studied. Result shows the reflectance reduction below 2% over a wide spectral range (500 – 1000 nm) for particle size 62.5 nm, period size 250 nm and gap 100 nm. Finally, PC1D data established *Isc* increased from 2.59 to 3.97 A along with photovoltaic efficiency of about 22.11%.

REFERENCES

1. R. Singh; *J. Nanophotonic*; 3 (1) 03203 (**2009**).
2. R. Sharma, A. Gupta and A. Virdi; *J. Nano-Electron. Phys.*; 9 (**2012**)
3. J. A. Dobrowolski, D. Poitras, P. Ma, H. Vakil, and M. Acree; *Applied Optics*; 41, 3075-83 (**2002**).
4. A. Deinega, I. Valuev, B. Potapkin and Y. Lozovik; *JOSA A*; 28, 770-7 (**2011**).
5. G. Hashmi, M. J. Rashid, Z. H. Mahmood, M. Hoq and M. H. Rahman; *J. Theoretical App. Phys.*; 12, 327 (**2018**).
6. S. Lien, D. Wun, W. Yeh and J. Liu; *Sol. Energ. Mat. Sol.Cells*; 90, 2710 (**2006**).
7. A. Bahrami, S. Mohammadnejad, N. J. Abkenar and S. Soleimaninezhad; *Int. J. Renew. Energ. Res.*; 3, 79 (**2013**).
8. M. Medhat, S. EL-Zaiat, S. Farag and G. Youssef; *Turkish Journal of Physics*; 40, 30 **(2016)**.
9. R. Sharma; *Turkish Journal of Physics*; 42, 350 (**2018**).
10. S. Pillai, K. R. Catchpole, T. Trupke and M. A. Green; *J. Appl. Phys.;* 101, 093105 (**2007**).
11. H. C. Lee, S. C. Wu, T. C. Yang, and T. J. Yen; *Energies*;3, 784-802 (**2010**).
12. D. M. Schaadt, B. Feng, and E. T. Yu; *Appl. Phys. Lett.*; 86, 063106 (**2005**).
13. D. Qu, F. Liu, J. Yu, W. Xie, Q. Xu, X. Li, and Y. Huang; *Appl. Phys. Lett.*; 98, 113119 (**2011**).
14. E. C. Wang, S. Mokkapati, T. Soderstrom, S. Varlamov and K. R. Catchpole; *IEEE J. Photovolt*; 3, 267-70 (**2013**).
15. T. L. Temple, G. D. K. Mahanama, H. S. Reehal and D. M. Bagnall; *Sol. Energy Mater. Sol. Cell*; 93, 1978-85 (**2009**).
16. H. A. Atwater, and A. Polman; *Nature Materials*; 9 (3), 205-13 (**2010**).
17. S. Link, Z. L. Wang, M. A. El-Sayed; *J. Phys. Chem. B*; 103(18), 3529-3533 (**1999**).
18. R. Sharma; *Heliyon (Elsevier)*; **5 (2019).**
19. H. A. Macleod; *Thin Film Optical Filters*, 2*nd* ed.; London Institute of Physics (**2001**).
20. M. F. Ubeid, M. M. Shabat, J. Charrier; *Romanian Report in Physics*; 72, 415 (2020).
21. M. A. Ordal, R. J. Bell, R. W. Alexander Jr., L. L. Long and M. R. Querry; *Applied optics*; 24, 4493 (**1983**).